IEEE Access
Multidisciplinary ⋮ Rapid Review ⋮ Open Access Journal

Received 20 February 2024, accepted 7 March 2024, date of publication 18 March 2024, date of current version 26 March 2024.

Digital Object Identifier 10.1109/ACCESS.2024.3379003

RESEARCH ARTICLE

Performance of a Neural Network Classifier Based Demodulator in Communication System

ANAND KUMAR, (Senior Member, IEEE)
Department of Electrical Engineering, School of Engineering Architecture Interior Design, Amity University Dubai, Dubai, United Arab Emirates
e-mail: akumar3@amityuniversity.ae

ABSTRACT The success rate of a neural network (NN) classifier (rectified linear unit, 10 layers, softmax output layer activation)-based demodulator was proposed and evaluated for phase-shift keying (PSK) and quadrature amplitude modulation (QAM) modulated signals corrupted by additive white Gaussian, chisquared, uniform, and Rayleigh noise channels with signal-to-noise ratios (SNR) ranging from -20 dB to +20 dB. Low SNR are common in spectrum sensing, cognitive radio networks, underwater acoustics, target detection, remote sensing, seismic monitoring, and helicopter blade detection. This classifier-demodulator performance was compared with that of the matched filter detector (MFD) for varying channel noise, constellation type (PSK or QAM), constellation size (M=2, 4, 8, 16), sample size (N), and training to test the data ratio. The classifier demodulator had a performance equal to or better than MFD in 98% of the scenarios. A training-to-test ratio of 70:30 or 80:20 is appropriate. The classifier performances of M-PSK and M-QAM are comparable. The superior performance of the NN classifier is more pronounced for M values greater than 2. N=5000 or higher is sufficient for most scenarios, and N=20000 is necessary for M=16. A higher success rate was obtained for additive chisquare and Rayleigh noise channels. The proposed demodulator performed significantly better than the matched filter for SNR values $\leq$ 0 dB. 16-QAM over an additive uniform noise channel has a better success rate for an SNR of 0 dB or less, whereas 16-QAM over an additive Rayleigh noise channel has a better success rate for an SNR of 5 dB or higher.

INDEX TERMS 6G mobile communications, quadrature amplitude modulation, phase shift keying, neural networks, AWGN channels, communication channels, matched filters.

I. INTRODUCTION

Communication systems were designed using rigorous mathematical frameworks. The mathematical framework does not account for imperfections in the systems and environment, and the consequent complex design of communication networks and systems. Deep Learning is being studied as an alternative that is less dependent on mathematical frameworks but more dependent on data patterns. These patterns were captured using the training data and applied to the test data.

Qin et al. [1] provided an overview of deep-learning (DL) methods for physical-layer communications. Feedforward neural networks (FNN) and recurrent neural networks (RNN) are considered. Farsad et al. [2] demonstrated that a deep neural network (DNN) results in a superior bit error rate (BER) compared to traditional methods in an environment with a signal-to-noise ratio (SNR) of 5–25 dB.

Kim et al. [3] designed new decoders for sequential codes (convolutional and turbo codes) that outperformed turbo decoders on nonadditive white Gaussian noise (non-AWGN) channels. The BER performance of their neural decoder was comparable to that of maximum likelihood (ML) (Viterbi) and maximum a posteriori (MAP). The training data have various combinations of 0 dB SNR, 100 sequence block

The associate editor coordinating the review of this manuscript and approving it for publication was Shadi Alawneh.

length, additive white Gaussian noise (AWGN) channel, and interleaving. The test data had combinations of SNR values in the range [−1 dB, +6 dB], 10000 sequence block lengths, and bursty noise channels.

Shi et al. [4] proposed a deep-learning-based automatic modulation recognition (AMR) method that distinguishes biphase phase-shift keying modulation (BPSK), quadrature phase-shift keying (QPSK), 8-phase shift keying (8-PSK), and 16-quadrature amplitude modulation (16-QAM) in the presence of channel noise ranging from −10 dB to 20 DB. The dataset comprised 20,000 samples, with 70% used for training and 30% used for testing the model.

Liu et al. [5] reviewed the developments in deep-learning-based physical layers. The limitations of conventional technologies include model accuracy, a lack of global optimality, and a lack of computational scalability. Deep learning (DL)-based signal-processing modules are model-free and are used in modulation recognition, channel estimation, channel state information (CSI) feedback, signal detection, and channel decoding. Typically, the architecture includes pre-processing, feature extraction, and classification.

Honkala et al. [6] proposed a deep fully CNN, DeepRx, which executes the full receiver pipeline in a 5G compliant fashion. This solution uses 3GPP-defined channel models in the signal-to-noise ratio (SNR) range of 0–20 dB. These findings indicate that the high performance of DeepRx can be attributed to temporal tracking of the channel, blind utilization of unknown data during the detection process, and advanced use of the data symbol distribution. This research demonstrates that higher performance for DeepRx is obtained when using channel models (Rayleigh) in training, which are different from the channel models (3GPP) used in the test data.

Hoydis et al. [7] explored the potential of Artificial Intelligence (AI) at a 6G air interface. A learned constellation at the transmitter side that is jointly optimized with the neural receiver with an approximately 3 dB improvement in BER over the baseline in the 5–20 dB SNR range.

Shea and Hoydis [8] applied ML techniques to the physical layer by viewing a communication system as an autoencoder. The architecture includes dense and normalization layers on the transmitter and receiver sides, and a noise layer for the channel. A linear rectified linear unit (ReLU), and softmax activation functions were used. MSE loss function is used. The Autoencoder had a comparable block error rate (BLER) performance over an SNR of 4–8 dB. The Autoencoder performed well for Rayleigh fading with noise of 0–20 dB. The performance of the CNN-based classification over a −20 dB to 20 dB noise level is presented, with a higher performance observed for 10 dB or more. The confusion matrix indicates that the classification is not able to clearly distinguish between 16-QAM and 64-QAM, and amplitude modulation (AM), double sideband (DSB), and wideband frequency modulation (WBFM).

Popoola and Olst [9] applied a neural network to sense the primary radio signals in a cognitive radio environment. The proposed multilayer feedforward neural network (MFFN) architecture extracts four features from a digitally modulated signal. This neural network has a success rate higher than 99.5% for five different modulation schemes (2ASK, 4ASK, 2FSK, BPSK, and QPSK) operating in channels with SNR ranging from −5 dB to 20 dB.

Zhang et al. [10] proposed a spectrum sensing method using clustering and signal features for cognitive wireless networks. The K-means and K-medoids algorithms were considered in this study. The detection performance is considered for SNR of −10 dB and −12 dB. We conclude that these three features are superior to those of energy use. However, the performance of a given feature depends on its conditions.

Lu et al. [11] used cooperative spectrum sensing in cognitive radio networks (CRN). A low-dimensional probability vector is used instead of an N-dimensional energy vector, which is required in a single primary user (PU) and N secondary user (SU) systems. 500-1000 samples were considered. The SVM-linear (probability vector) has the best performance, 'High' probability of detection, 'Low' training duration and 'Low' classification delay.

Fig 1 shows a basic communication system model comprising a transmitter, receiver, and additive white Gaussian noise (AWGN) channel. The transmitter includes a modulation module: M-Phase Shift Keying (M-PSK) modulation and M-Quadrature Amplitude Modulation (M-QAM) were considered in this work. For PSK, M=2, 4, 8, and 16 was considered, whereas for QAM, M=2, 4, 8, and 16 was considered. SNR values of −20, −10, −5, 0, 5, 10, and 20 dB were considered. The receiver is a hard decision demodulator (matched filter detection) for M-PSK, a hard decision demodulator (matched filter detection) for M-QAM, or a neural network-based classifier.

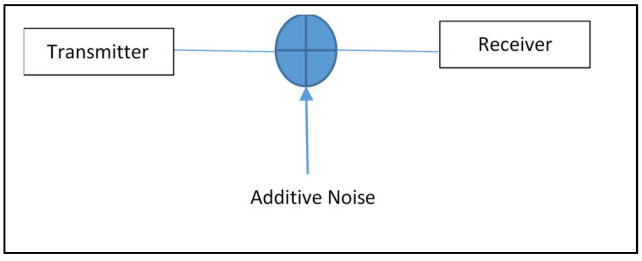

FIGURE 1. Basic communication system that comprises of a transmitter, additive channel noise and receiver. The transmitter is one of the following: M-PSK modulation or M-QAM. The additive noise could be additive white Gaussian noise (AWGN) or additive non-Gaussian (chisquared, uniform, Rayleigh) noise. The receiver is one of the following M-PSK or M-QAM demodulator (matched filter detector) or NN classifier.

Many prior studies have analyzed the performance of neural network demodulator solutions for an SNR of 0 dB or more. Typically, CRNs operate at an SNR of less than 0 dB. In this study, the performance of a neural network classifier was studied from −20 dB to +20 dB over additive

white Gaussian noise (AWGN) and additive non-Gaussian (Chisquared, Uniform, and Rayleigh) channels.

The performance of a neural network-based classifier for an M-PSK-modulated noisy signal was compared for various constellations (M = 2, M = 4, M=8, and M = 16). Similarly, the performance of the neural network classifier for an M-QAM-modulated noisy signal is compared for various constellations (M = 2, M = 4, M = 8, and M = 16).

The performance of the neural network classifier demodulator for an M-PSK-modulated noisy signal was compared with that of the demodulator for an M-QAM-modulated noisy signal.

In this study, the performance of a neural network classifier was investigated for sample sizes of 100, 200, 1000, 5000, 10000, and 20000. Furthermore, the training-to-test sample size ratios of 60:40, 70:30, and 80:20 were considered.

II. RESULTS AND DISCUSSION

The following parameters were used to define the neural network for the classifier used in this study.

TABLE 1. Parameters of neural network classifier.

S. No.	Type	Parameters/Values/Examples
1	Input, Output of NN-based classifier	Input: Output of noise channel – Two input vectors Output: One output vector
2	Symbol/Class Name	Example: [0 1 2 3 4 5 6 7] for M=8
3	Number of samples/observations	N=100,200,1000,5000,10000, 20000
4	Number of Layers	10
5	Activation Layer	Rectified Layer unit (ReLU)
6	Output Layer Activation	softmax
7	Ratio of training to test data	60:40, 70:30,80:20

Bit error rate (BER) is often used to determine communication performance. However, there is a need to compare the performance of the NN-based demodulator with that of traditional demodulators; in this study, the Symbol Error Rate is used with a nomenclature of ''Success Rate, Percentage'' of successful demodulation of a given symbol transmitted over a given channel. The rate was calculated as the average of 100 repetitions for a given value of M (2, 4, 8, or 16) for a given sample size (100, 200, 1000, 5000, 10000 or 20000), and for a particular SNR (−20, −10, −5, 0, 5, 10, or 20).

In Fig 2, the success rate (percentage) is plotted for M=2, M=4, M=8, and M=16, 20000 samples for SNR values ranging from -20 dB to 20 dB. The plots are for the hard-decision PSK demodulator (matched filter detection) and NN-based demodulator following the PSK modulation and AWGN channels. From the initial analysis, the plots were similar for the training and test data at ratios of 60:40, 70:30, and 80:20 for a given value of M. One arrived at this conclusion by a visual comparison of Fig 2 with Fig 3 and Fig 4, which

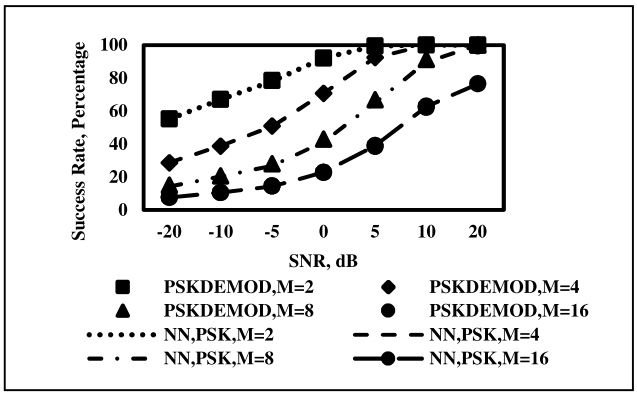

FIGURE 2. Success rate (percentage) is plotted for M=2, M=4, M=8, M=16 for N=20000 for SNR values from −20 dB to 20 dB. The success rate for the hard decision PSK demodulator (matched filter detection) and the Neural Network based demodulator following PSK modulation and the AWGN channel, is plotted. The graph is plotted for training and test data in the ratio of 70:30. Each data point is based on 100 repetitions.

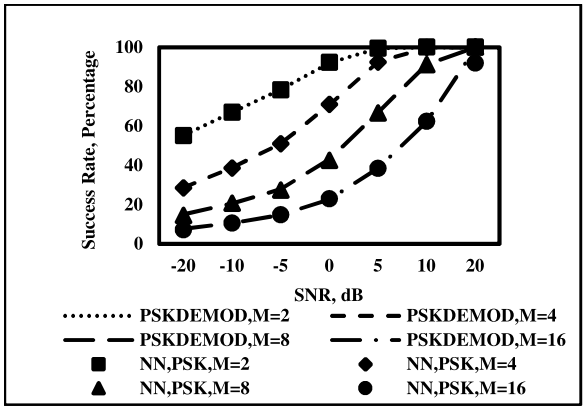

FIGURE 3. Success rate (percentage) is plotted for M=2, M=4, M=8, M=16 for N=20000 for SNR values from −20 dB to 20 dB. The success rate for hard decision PSK demodulator (matched filter detection) and a Neural Network based demodulator following PSK modulation and the AWGN channel, is plotted. The training and the test data are in the ratio of 60:40. Each data point is based on 100 repetitions.

are plotted for training to test data in the ratios of 60:40 and 80:20, respectively, for the PSK demodulator and NN-based demodulator for different values of M and N=20000. Each data point is an average of 100 repetitions. It is further observed that the success rate, in general, for a given value of SNR, is highest for M=2 and lowest for M=16, until for higher values of SNR, the success rate ceils at 100%. A more detailed analysis is presented in Section III based on the data presented in Table 6.

In Fig 5, the success rate (percentage) is plotted for M=2, M=4, M=8, and M=16, 20000 samples for SNR values ranging from -20 dB to 20 dB. The plots are almost identical for the hard decision QAM demodulator (matched filter detection) and the NN-based demodulator, following the QAM and AWGN channels, for a given value of M. From the initial analysis, the plots appear similar for training and test data in the ratios of 60:40, 70:30, or 80:20 for a given value of

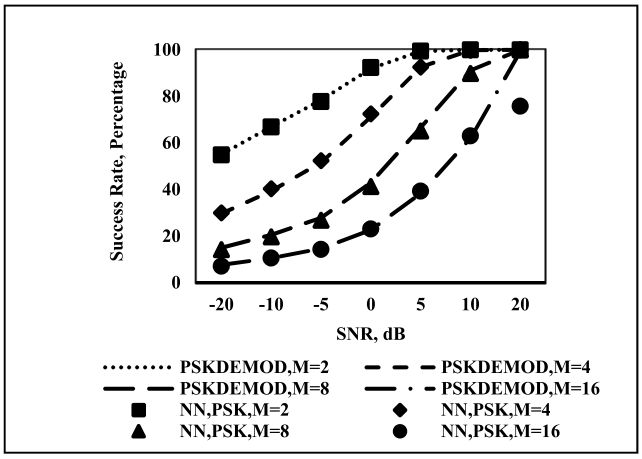

FIGURE 4. Success rate (percentage) is plotted for M=2, M=4, M=8, M=16 for N=20000 for SNR values from −20 dB to 20 dB. The success rate for hard decision PSK demodulator (matched filter detection) and a Neural Network based demodulator following PSK modulation and the AWGN channel, is plotted. The Training and Test data are in the ratio of 80:20. Each data point is based on 100 repetitions.

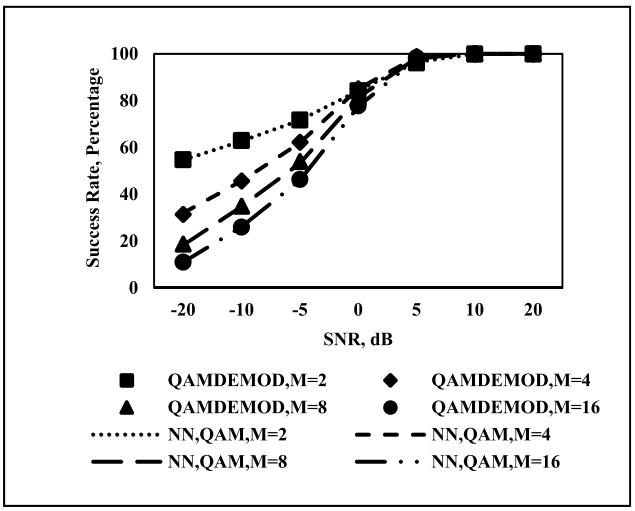

FIGURE 5. Success rate (percentage) is plotted for M=2, M=4, M=8, M=16 for N=20000 for SNR values from −20 dB to 20 dB. The success rate for hard decision QAM demodulator (matched filter detection) and a Neural Network based demodulator, following QAM and the AWGN channel, is plotted. The Training and Test data are in the ratio of 70:30. Each data point is based on 100 repetitions.

M; one arrives at this conclusion by a visual comparison of Fig 5 with Fig 6 and Fig 7, which are plotted for training to test data in the ratios of 60:40 and 80:20, respectively, for the QAM demodulator and the NN-based demodulator for different values of M and N=20000. Each data point is an average of 100 repetitions. It is further observed that the success rate, in general, for a given value of SNR, is highest for M=2 and lowest for M=16, until for higher values of SNR, the success rate ceils at 100%. A more detailed analysis is presented in Section III based on the data presented in Table 6.

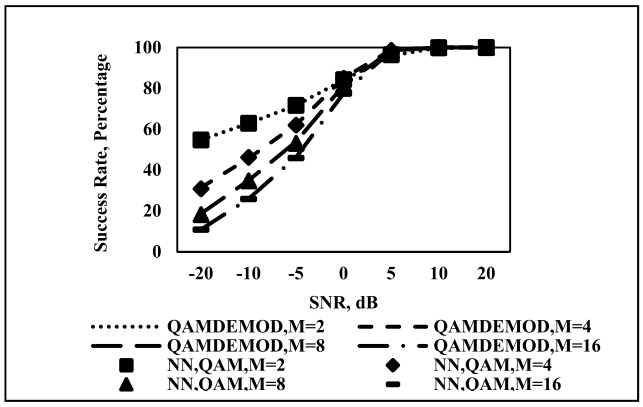

FIGURE 6. Success rate (percentage) is plotted for M=2, M=4, M=8, M=16 for N=20000 for SNR values from −20 dB to 20 dB. The success rate for hard decision QAM demodulator (matched filter detection) and a Neural Network based demodulator following QAM and the AWGN channel, is plotted. The training and the test data are in the ratio of 60:40. Each data point is based on 100 repetitions.

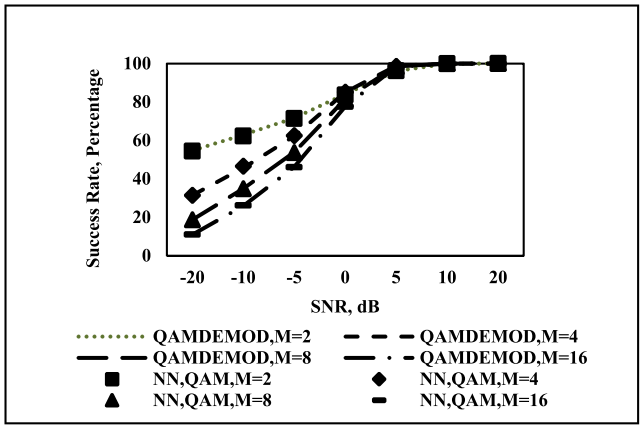

FIGURE 7. Success rate (percentage) is plotted for M=2, M=4, M=8, M=16 for N=20000 for SNR values from −20 dB to 20 dB. The success rate for the hard decision QAM demodulator (matched filter detection) and a Neural Network based demodulator following QAM and the AWGN channel, is plotted. The training and the test data are in the ratio of 80:20. Each data point is based on 100 repetitions.

Based on the analysis in Section III, subsequent simulations in this study used a training-to-test ratio of 70:30.

The relationship between the success rate curves for various values of M is similar for each of the following cases, with the success rate for a given SNR being the highest for M=2 and the lowest for M=16:

1) NN demodulator following PSK modulation, AWGN channel
2) NN demodulator following QAM, AWGN channel
3) Hard decision PSK demodulator (matched filter detection) following PSK modulation, AWGN channel
4) Hard decision QAM demodulator (matched filter detection) following QAM, AWGN channel

For AWGN, the generalized likelihood ratio test (matched filter detection) is optimal [12]. The SNR is maximized when a matched filter is used with a stationary white noise

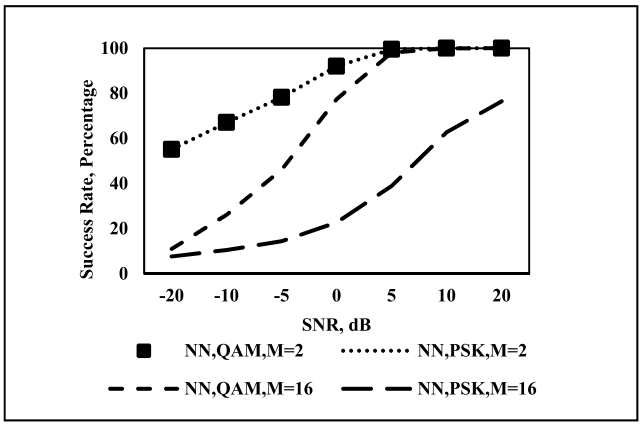

FIGURE 8. Success rate (percentage) is plotted for M=2, N=20000 samples and M=16, N=20000 samples for SNR values from −20 dB to 20 dB. The ratio of the training data to the test data was 70:30. The success rate curves for NN-based demodulator following QAM and the AWGN channel and NN-based demodulator following PSK modulation and the AWGN channel are plotted for M=2 and M=16.

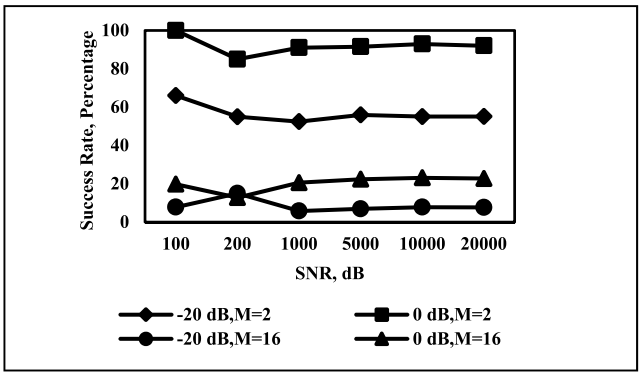

FIGURE 9. Success rate (percentage) is plotted for M=2 and M=16 against number of sample sizes of N=100, 200, 1000, 5000, 10000 and 20000 for SNR values of −20 dB and 0 dB for AWGN. The ratio of the training data to the test data was 70:30. The success rate curves are for the NN-based demodulator following PSK modulation and the AWGN channel. Each data point is an average of 100 repetitions.

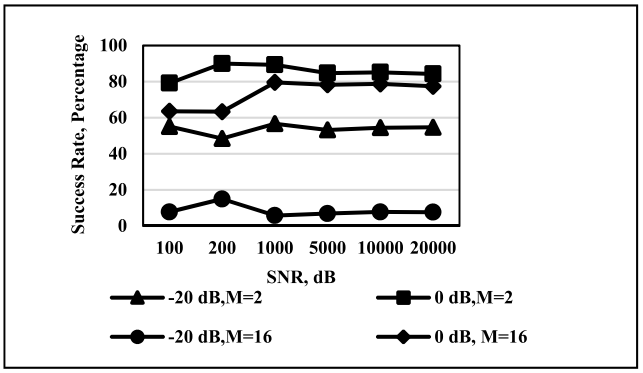

FIGURE 10. Success rate (percentage) is plotted for M=2 and M=16 against number of sample sizes of N=100, 200, 1000, 5000, 10000 and 20000 for SNR values of −20 dB and 0 dB. The ratio of the training data to the test data is 70:30. The success rate curves are for NN-based demodulator following QAM and the AWGN channel. Each data point is an average of 100 repetitions.

channel [14]; hence, the matched filter detector is optimal. The simulation results confirm that the NN-based demodulator is not superior to the optimal detector. However, they also confirmed that the NN-based demodulator was as effective as an optimal detector.

In Fig 8, the success rates are plotted against the SNR (dB) for M=2 and M=16 for N=20000 samples. The training-to-test data ratio is 70:30. The values of the SNR range from −20 dB to +20 dB. The performance of the NN-based modulator following PSK modulation and the AWGN channel is identical to that of the NN-based demodulator following QAM and AWGN channels for M=2. For M=16, the performance of the NN-based demodulator following the QAM and AWGN channels was significantly higher than that of the NN-based demodulator following PSK modulation and the AWGN channel for 0 dB or less. This suggests that the NN-based demodulator depends on the constellation used in the modulation type. Similar performance divergence was observed for M=4 and M=8.

In Figs. 9 and 10, the success rate is plotted for various sample sizes (N = 200, 1000, 5000, 10000 and 20000). The success rate of the NN-based demodulator following the PSK and AWGN channels is plotted in Fig 9 for SNR values of -20 B and 0 dB, and M=2, 16. In Fig 10, the success rates are plotted for the NN-based demodulator following QAM and AWGN channels. The ratio of the training to test data was 70:30. Although the success rates vary with sample size, there seems to be no visible trend of constant increase in the success rate based on the sample size. A more detailed analysis is presented in Section III based on the data presented in Table 5.

A matched filter detector is not optimal for non-Gaussian noise channels [15], [16]. Hence, a comparative study on the performance of NN-based demodulators was conducted for additive non-Gaussian (chisquared, uniform, and Rayleigh) channels. Additive non-Gaussian noise was generated for an appropriate SNR, similar to the generation of AWGN [13].

A. ADDITIVE CHISQUARED NOISE CHANNEL

In Fig 11, the success rate (percentage) is plotted for M=2, 4, 8, and 16 against SNR values of -20 dB to 20 dB for N=20000. The ratio of the training data to test data was 70:30. The success rate curves are for the hard-decision PSK demodulator (matched filter detection) and NN-based demodulator, following the PSK modulation and an additive chisquared noise channel. Each data point is an average of 100 repetitions. The relationship between the success rate curves for various values of M is very similar for the same demodulator when used with the AWGN channel, with the success rate for a given SNR being highest for M=2 and lowest for M=16 (compared with Fig 2). As with the matched filter demodulator, the NN-based demodulator has a significant dependence on parameter M used in the M-PSK modulation. Furthermore, the performance of the NN-based demodulator was superior to that of the matched filter-detection demodulator for a given value of M for lower

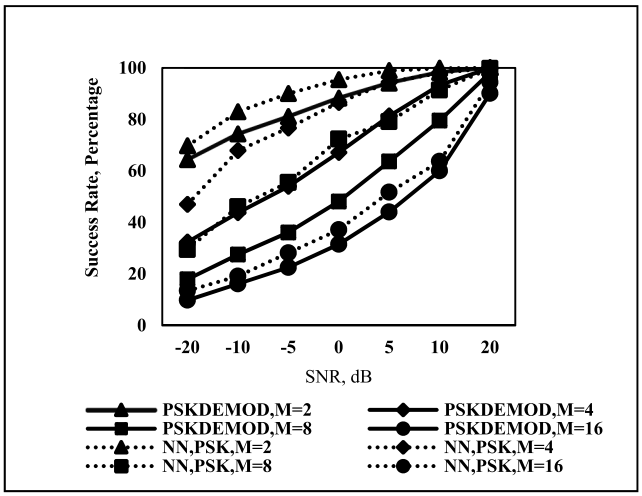

FIGURE 11. Success rate (percentage) is plotted for M=2, 4, 8, 16 against SNR values of −20 dB to 20 dB for N=20000. The ratio of the training data to the test data was 70:30. The success rate curves are for the hard decision PSK demodulator (matched filter detection) and NN-based demodulator, following PSK and the additive Chisquared noise channel. Each data point is an average of 100 repetitions.

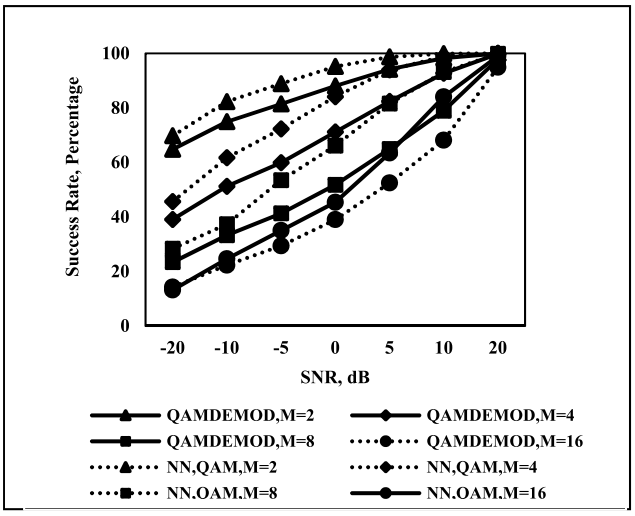

FIGURE 12. Success rate (percentage) is plotted for M=2, 4, 8, 16 against SNR values of −20 dB to 20 dB for N=20000. The ratio of the training data to the test data is 70:30. The success rate curves are for hard decision QAM demodulator (matched filter detection) and NN-based demodulator, following QAM and the additive Chisquared noise channel. Each data point is an average of 100 repetitions.

SNR values. The NN demodulator performed well for all the SNR values.

In Fig. 12, the success rate (percentage) is plotted for M=2, 4, 8, and 16 against SNR values of -20 dB to 20 dB for N=20000. The ratio of the training data to test data was 70:30. The success rate curves are for the hard-decision QAM demodulator (matched filter detection) and NN-based demodulator, following the QAM and an additive-chisquared noise channel. Each data point is an average of 100 repetitions. The relationship between the success rate curves for various values of M is very similar for the same demodulator

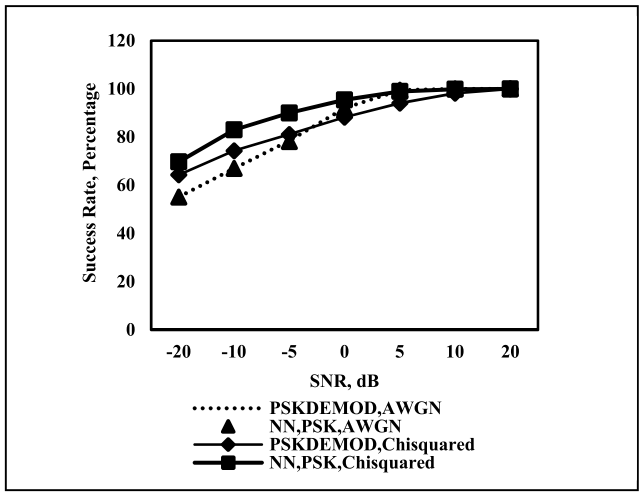

FIGURE 13. Success rate (percentage) is plotted for M=2 against SNR values of -20 dB to 20 dB for N=20000. The ratio of the training data to the test data was 70:30. The success rate curves are for hard decision PSK demodulator (matched filter detection) and NN-based demodulator following PSK modulation and the additive chisquared noise channel. The success rates are also plotted for the AWGN channel. Each data point is an average of 100 repetitions.

when used with the AWGN channel, with the success rate for a given SNR being the highest for M=2 and the lowest for M=16 (compared with Fig 5). As with the matched filter demodulator, the NN-based demodulator has a significant dependence on parameter M used in the M-PSK modulation. Furthermore, the performance of the NN-based demodulator was superior to that of the matched filter-detection demodulator for a given value of M for lower SNR values. The NN demodulator performed well for all the SNR values.

In Fig 13, the success rate (percentage) is plotted for M=2 against SNR values of -20 dB to 20 dB for N=20000. The ratio of the training data to test data was 70:30. The success rate curves are for the hard-decision PSK demodulator (matched filter detection), NN-based demodulator following PSK modulation, and the additive chisquared noise channel. The success rate curves for the AWGN channel are identical for the PSK demodulator and the NN-based demodulator. Each data point is an average of 100 repetitions. Clearly, the success rate curves for the additive non-Gaussian (chisquared) channel differ from those for the AWGN channel. It was also observed that the NN-based demodulator consistently outperformed the matched-filter-detection-based demodulator for lower SNR values in this non-Gaussian channel. The NN demodulator performed well for all the SNR values. This observation extends to the same demodulator and modulation characteristics when M=16 (Fig 14). Similarly, the performance of the NN-based modulator was superior to that of the matched filter detection-based demodulator following the QAM and additive chisquared noise channel for both M = 2 (Fig 15) and M = 16 (Fig 16) for lower SNR values. The NN demodulator performed well for all the SNR values. Furthermore, both the matched filter detector and NN-based classifier demodulator performance for the

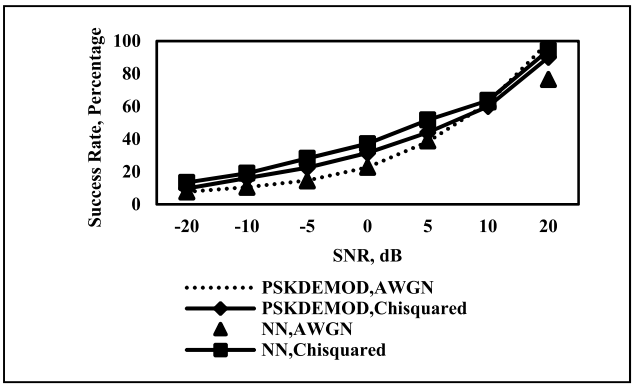

FIGURE 14. Success rate (percentage) is plotted for M=16 against SNR values of −20 dB to 20 dB for N=20000. The ratio of the training data to the test data was 70:30. The success rate curves are for hard decision PSK demodulator (matched filter detection) and NN-based demodulator following PSK modulation and the additive Chisquared noise channel. The success rates are also plotted for the AWGN channel. Each data point is an average of 100 repetitions.

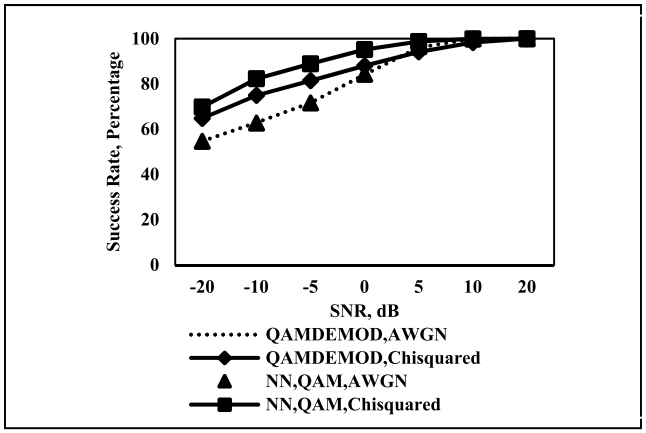

FIGURE 15. Success rate (percentage) is plotted for M=2 against SNR values of −20 dB to 20 dB for N=20000. The ratio of the training data to the test data was 70:30. The success rate curves are for the hard decision QAM demodulator (matched filter detection) and NN-based demodulator following QAM and the additive chisquared noise channel. The success rates are also plotted for the AWGN channel. Each data point is an average of 100 repetitions.

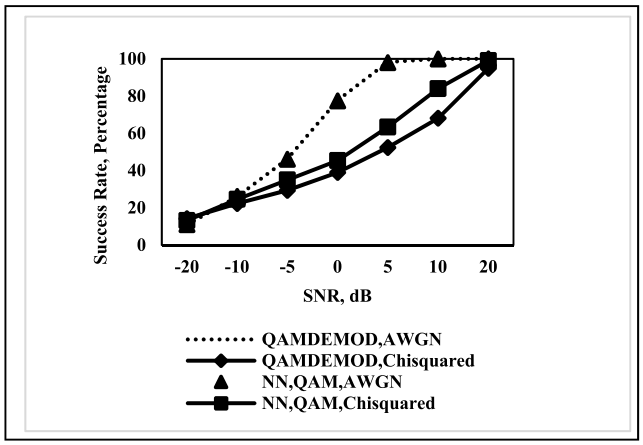

FIGURE 16. Success rate (percentage) is plotted for M=16 against SNR values of −20 dB to 20 dB for N=20000. The ratio of the training data to the test data is 70:30. The success rate curves are for hard decision QAM demodulator (matched filter detection) and NN-based demodulator following QAM and the additive chisquared noise channel. The success rates are also plotted for the AWGN channel. Each data point is an average of 100 repetitions.

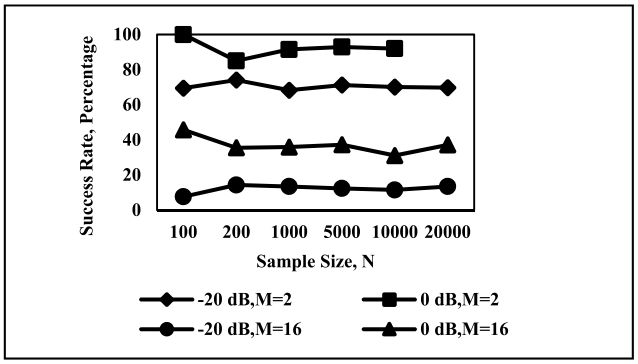

FIGURE 17. Success rate (percentage) is plotted for M=2 and M=16 against number of sample sizes of N=100, 200, 1000, 5000, 10000 and 20000 for SNR values of −20 dB and 0 dB for the chisquared channel. The ratio of the training data to the test data was 70:30. The success rate curves are for NN-based demodulator following PSK modulation and the additive chisquared channel. Each data point is an average of 100 repetitions.

additive chisquare channel exceeded the performance of these detectors for the AWGN channel for many SNR values, except 16-QAM (Figs 13-16).

In Figs. 17 and 18, the success rate is plotted for various numbers of samples (N = 200, 1000, 5000, 10000, and 20000). The success rate of the NN-based demodulator following PSK modulation and the additive chisquared channel is plotted in Fig 17 for SNR values of -20 B and 0 dB and M=2, 16. In Fig 18, the success rates are plotted for the NN-based demodulator following the QAM and additive chisquare channels. The ratio of the training to test data was 70:30. Although the success rates vary with sample size, there seems to be no visible trend of a constant increase in the success rate with sample size. A more detailed analysis is presented in Section III based on the data presented in Table 5.

B. ADDITIVE UNIFORM NOISE CHANNEL

In Fig 19, the tted for M=2 against SNR values of -20 dB to 20 dB for N=20000. The ratio of the training data to test data was 70:30. The success rate curves are for the hard-decision PSK demodulator (matched filter detection) and NN-based demodulator following PSK modulation and the additive uniform-noise channel. The success rate curves for the AWGN channel are identical for the PSK demodulator and the NN-based demodulator. Each data point is an average of 100 repetitions. Clearly, the success rate curves for the additive non-Gaussian (uniform) channel are different from those for the AWGN channel. It was also observed that the NN-based demodulator consistently outperformed the matched-filter-detection-based demodulator for lower SNR values in this non-Gaussian channel. The NN demodulator performed well for all the SNR values. This observation

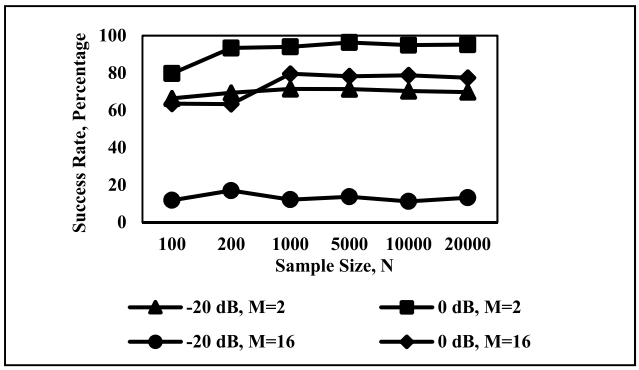

FIGURE 18. Success rate (percentage) is plotted for M=2 and M=16 against number of sample sizes of N=100, 200, 1000, 5000, 10000 and 20000 for SNR values of −20 dB and 0 dB for chisquared channel. The ratio of the training data to the test data was 70:30. The success rate curves are for the NN-based demodulator following QAM and the additive chisquared channel. Each data point is an average of 100 repetitions.

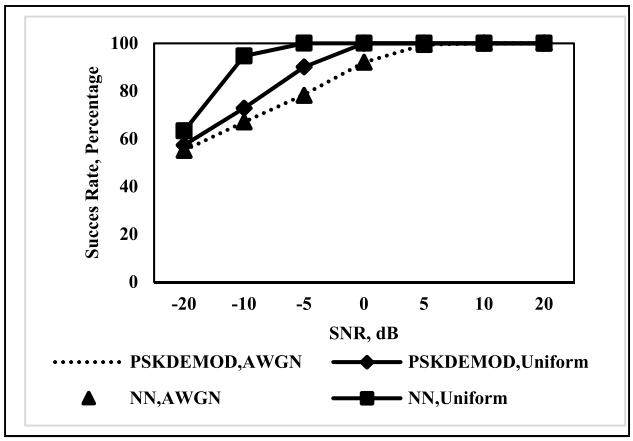

FIGURE 19. Success rate (percentage) is plotted for M=2 against SNR values of −20 dB to 20 dB for N=20000. The ratio of the training data to the test data was 70:30. The success rate curves are for the hard decision PSK demodulator (matched filter detection) and the NN-based demodulator following PSK modulation and the additive uniform noise channel. The success rates are also plotted for the AWGN channel. Each data point is an average of 100 repetitions.

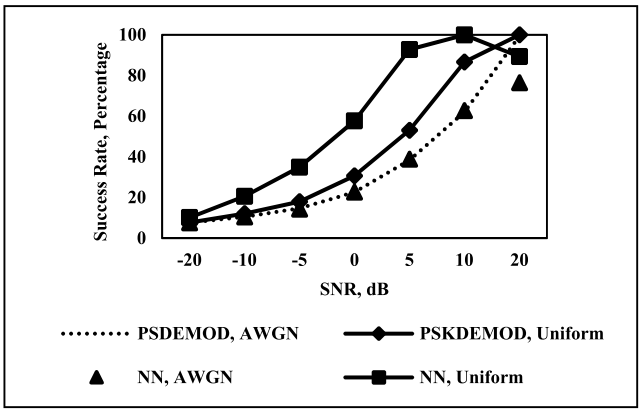

FIGURE 20. Success rate (percentage) is plotted for M=16 against SNR values of −20 dB to 20 dB for N=20000. The ratio of the training data to the test data was 70:30. The success rate curves are for the hard decision PSK demodulator (matched filter detection) and the NN-based demodulator following PSK modulation and the additive uniform noise channel. The success rates are also plotted for the AWGN channel. Each data point is an average of 100 repetitions.

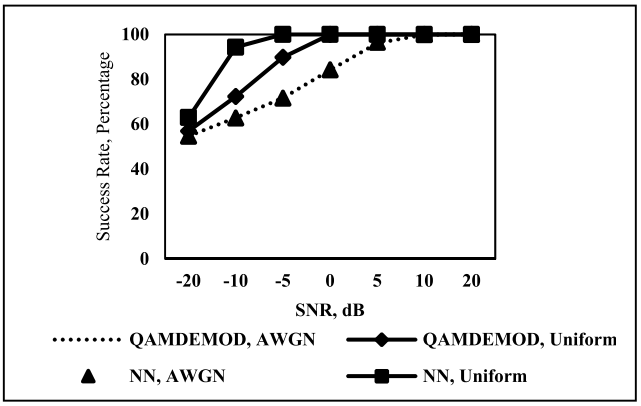

FIGURE 21. Success rate (percentage) is plotted for M=2 against SNR values of −20 dB to 20 dB for N=20000. The ratio of the training data to the test data was 70:30. The success rate curves are for the hard decision QAM demodulator (matched filter detection) and the NN-based demodulator following QAM and the additive uniform noise channel. The success rates are also plotted for the AWGN channel. Each data point is an average of 100 repetitions.

extends to the same demodulator and modulation characteristics for M=16 (Fig 20). Similarly, the performance of the NN-based demodulator was superior to that of the matched-filter-detection-based demodulator following the QAM and the additive uniform noise channel for both M = 2 (Fig 21) and M =16 (Fig 22) at lower SNR values. The NN demodulator performed well for all the SNR values. Furthermore, both the matched filter detector and NN-based classifier demodulator performance for the additive uniform channel exceeded the performance of these detectors for the AWGN channel for many SNR values, except 16-QAM (Figs 19-22).

C. ADDITIVE RAYLEIGH NOISE CHANNEL

In Fig 25, the success rate (percentage) is plotted for M=2 against SNR values of -20 dB to 20 dB for N=20000. The ratio of the training data to test data was 70:30. The success rate curves are for the hard-decision PSK demodulator (matched filter detection) and NN-based demodulator following PSK modulation and the additive Rayleigh noise channel. The success rate curves for the AWGN channel are identical for the PSK demodulator and the NN-based demodulator. Each data point is an average of 100 repetitions. Clearly, the success rate curves for the additive non-Gaussian (Rayleigh) channel differed from those for the AWGN channel. It was also observed that the NN-based demodulator outperformed the matched-filter-detection-based demodulator for lower SNR values in a non-Gaussian channel. The NN demodulator performed well for all the SNR values. This observation extends to the same demodulator and modulation characteristics for M=16 (Fig 26). Similarly, the performance of the NN-based demodulator was superior to that of the matched-filter-detection-based demodulator following the QAM and additive Rayleigh noise channel for both M = 2 (Fig 27) and

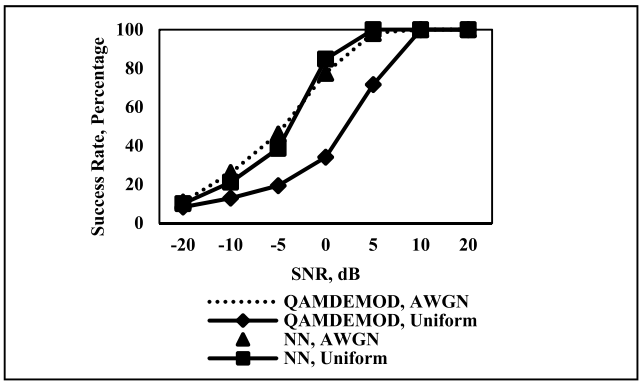

FIGURE 22. Success rate (percentage) is plotted for M=16 against SNR values of −20 dB to 20 dB for N=20000. The ratio of the training data to the test data was 70:30. The success rate curves are for the hard decision QAM demodulator (matched filter detection) and the NN-based demodulator following QAM and the additive uniform noise channel. The success rates are also plotted for the AWGN channel. Each data point is an average of 100 repetitions.

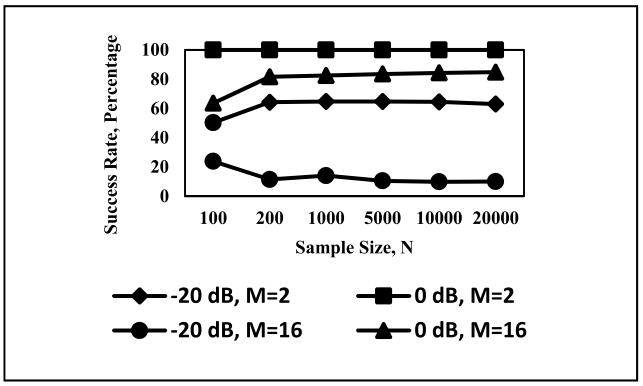

FIGURE 24. Success rate (percentage) is plotted for M=2 and M=16 against number of sample sizes of N=100, 200, 1000, 5000, 10000 and 20000 for SNR values of −20 dB and 0 dB for Uniform channel. The ratio of the training data to the test data was 70:30. The success rate curves are for the NN-based demodulator following QAM and the additive uniform channel. Each data point is an average of 100 repetitions.

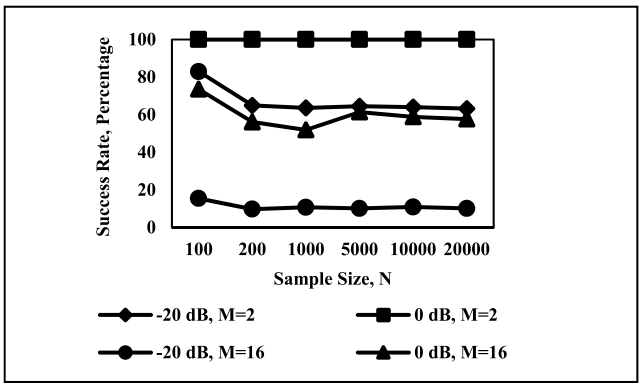

FIGURE 23. Success rate (percentage) is plotted for M=2 and M=16 against the number of sample sizes of N=100, 200, 1000, 5000, 10000 and 20000 for SNR values of −20 dB and 0 dB for uniform channel. The ratio of the training data to the test data was 70:30. The success rate curves are for the NN-based demodulator following PSK modulation and the additive uniform channel. Each data point is an average of 100 repetitions.

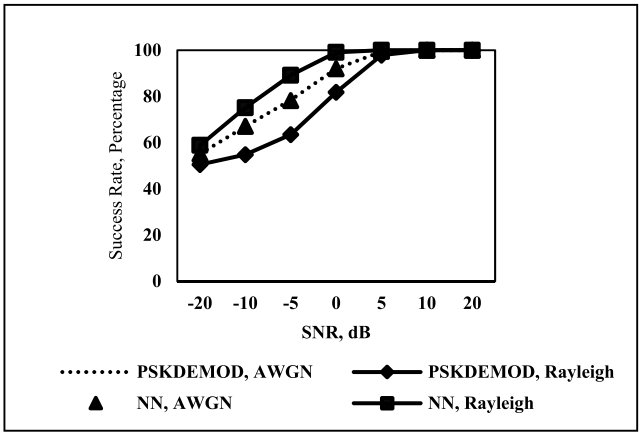

FIGURE 25. Success rate (percentage) is plotted for M=2 against SNR values of −20 dB to 20 dB for N=20000. The ratio of the training data to the test data was 70:30. The success rate curves are for hard decision PSK demodulator (matched filter detection) and NN-based demodulator following PSK modulation and the additive Rayleigh noise channel. The success rates are also plotted for the AWGN channel. Each data point is an average of 100 repetitions.

M =16 (Fig 28) for lower SNR values. The NN demodulator performed well for all the SNR values. Furthermore, for many SNR values, both the matched filter detector and NN-based classifier demodulator performance for the AWGN channel lie between the performances of the NN-based classifier and matched filter detector for the Rayleigh channel, except for 16-QAM (Figs 25-28), for many SNR values.

In Figs. 29 and 30, the success rate is plotted for various sample sizes (N = 200, 1000, 5000, 10000, and 20000, respectively). The success rate of the NN-based demodulator following PSK modulation and the additive uniform channel is plotted in Fig 30 for SNR values of -20 B and 0 dB, and M=2, 16. In Fig 31, the success rates are plotted for the NN-based demodulator following the QAM and additive uniform channels. The ratio of the training to test data was 70:30. Although the success rates vary with sample size, there seems to be no visible trend of a constant increase in the success rate with sample size. A more detailed analysis is presented in Section III based on the data presented in Table 5.

III. COMPREHENSIVE ANALYSIS AND SUMMARY OF FINDINGS

The signal, modulation, noise channel, and neural-network-classifier-based demodulator parameters and specifications are listed in Table 2.

The signal comprises N uniformly distributed pseudorandom integers in the range [0, M-1] where N takes on values in the range {100, 200, 1000, 5000, 10000, 20000). PSK and QAM were used with M = 2, 4, 8, and 16. AWGN, additive chisquared noise, additive uniform noise, and additive Rayleigh noise channels are considered. SNR takes on values of −20 dB, −10 dB, −5 dB, 0 dB, 5 dB, 10 dB and 20 dB. The first fully connected layer used a rectified linear unit (ReLU)

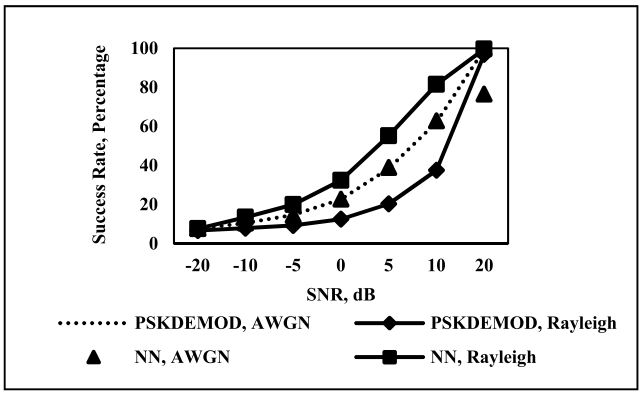

FIGURE 26. Success rate (percentage) is plotted for M=16 against SNR values of −20 dB to 20 dB for N=20000. The ratio of the training data to the test data was 70:30. The success rate curves are for the hard decision PSK demodulator (matched filter detection) and NN-based demodulator following PSK modulation and the additive Rayleigh noise channel. The success rates are also plotted for the AWGN channel. Each data point is an average of 100 repetitions.

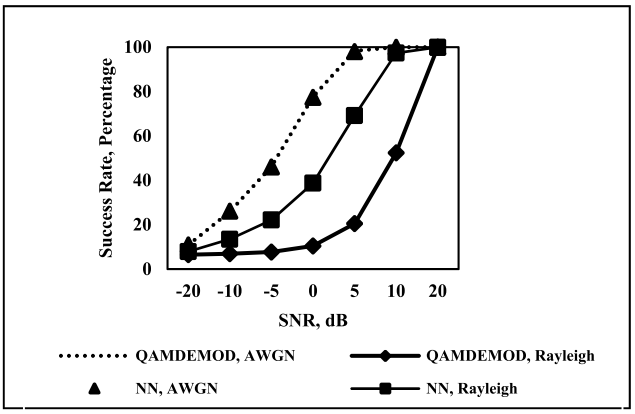

FIGURE 28. Success rate (percentage) is plotted for M=16 against SNR values of −20 dB to 20 dB for N=20000. The ratio of the training data to the test data was 70:30. The success rate curves are for the hard decision QAM demodulator (matched filter detection) and the NN-based demodulator following QAM and the additive Rayleigh noise channel. The success rates are also plotted for the AWGN channel. Each data point is an average of 100 repetitions.

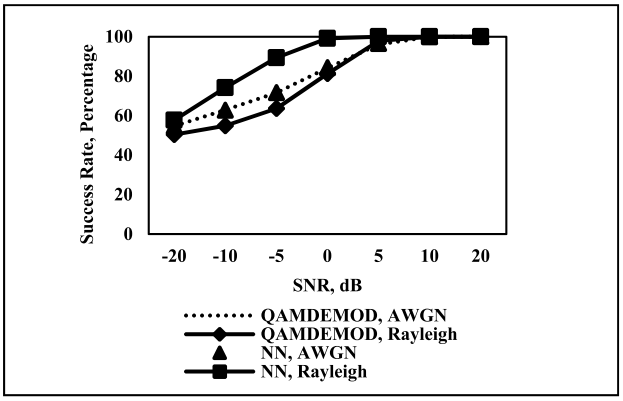

FIGURE 27. Success rate (percentage) is plotted for M=2 against SNR values of −20 dB to 20 dB for N=20000. The ratio of the training data to the test data was 70:30. The success rate curves are for the hard decision QAM demodulator (matched filter detection) and the NN-based demodulator following QAM and the additive Rayleigh noise channel. The success rates are also plotted for the AWGN channel. Each data point is an average of 100 repetitions.

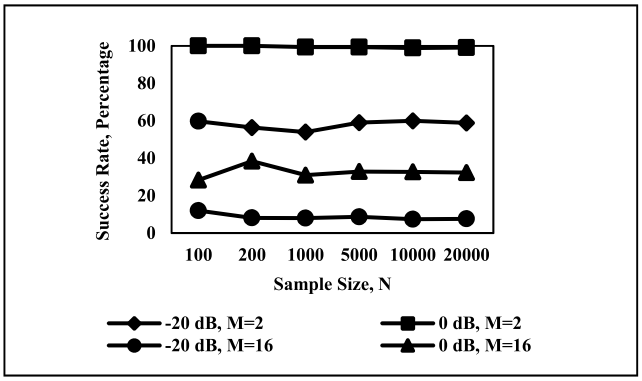

FIGURE 29. Success rate (percentage) is plotted for M=2 and M=16 against number of sample sizes of N=100, 200, 1000, 5000, 10000 and 20000 for SNR values of −20 dB and 0 dB for additive Rayleigh channel. The ratio of the training data to the test data was 70:30. The success rate curves are for the NN-based demodulator following PSK modulation and the additive Rayleigh channel. Each data point is an average of 100 repetitions.

activation function, which consisted of 10 layers, and the final fully connected layer used a Softmax activation function.

The performances of the optimal detector and the neural network classifier are compared in Table 3. The performance of the proposed demodulator was identical to that of a matched filter detector for a given modulator type with an AWGN channel. The only deviation observed was for the 16-PSK at an SNR of 20 dB.

Table 2 presents the channel parameters considered in this study, which list the additive non-Gaussian channels: chisquared, uniform, and Rayleigh. The performance of the neural-network classifier demodulator for different channel types is presented in Table 4 as the difference between the success rate of the proposed demodulator and that of the matched filter for the same signal, modulation, and noise channel parameters. An ad hoc value of 5% is a measure of the superiority of the proposed demodulator over the matched filter, which cannot be attributed to the lack of significant variations. The analysis of the data in the table leads to the following conclusions.

1) The proposed demodulator is superior to the matched filter detector for all modulators, except for a minor and perhaps insignificant deviation for 16-QAM (-20 dB) with an additive chisquared noise channel and 16-QAM (20 dB) in an additive uniform channel. The other deviation from this conclusion is for 16-PSK (20 dB) in the additive Rayleigh noise channel, which is interesting because the SNR of 20 dB is quite high, and the performance of the matched filter detector is superior. This translates to 0.02% in the scenarios listed in Table 3.

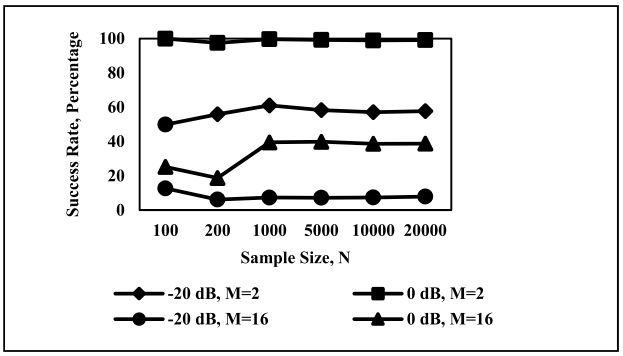

FIGURE 30. Success rate (percentage) is plotted for M=2 and M=16 against number of sample sizes of N=100, 200, 1000, 5000, 10000 and 20000 for SNR values of −20 dB and 0 dB for the additive Rayleigh channel. The ratio of the training data to the test data was 70:30. The success rate curves are for the NN-based demodulator following QAM and the additive Rayleigh channel. Each data point is an average of 100 repetitions.

TABLE 2. Signal, modulator, channel and NN receiver parameters and specifications.

Signal	Modulation	Noise channel	NN demodulator
			Two inputs from Noise Channel
			Symbol/Class Name in {0,1,2,3,4,5,6,7}
			Value of M
			Value of N
			Number of Outputs of First Fully Connected Layer: 10
			Activation Layer of First Fully Connected Layer: ReLU $f(x) = x, x \geq 0$ $0, x \leq 0$
Uniformly distributed pseudorandom integers in the range [0,M-1]	Constellation Type: PSK, QAM	Channel Type: AWGN, additive non-Gaussian channel (Chisquared, Uniform, Rayleigh)	
Sample Size, N in the range {100, 200, 1000, 5000, 10000, 20000}	Constellation Size, M in the range {2, 4, 8, 16}	SNR (dB) with values in {-20, -10, -5, 0, 5, 10 20}	Number of Layers = 10
			Final Fully Connected Layer Activation Layer: softmax $f(x_i) = \frac{\exp(x_i)}{\sum_{j=1}^{K} \exp(x_j)}$
			Number of outputs of Final Fully Connected Layer: K = M
			Ratio of Training:Test data in {60:40, 70:30, 80:20}

2) In 100 out of 168 or 60% of the scenarios in Table 4, the success rate of the neural network classifier demodulator exceeded that of the matched filter detector for additive non-Gaussian channels with an SNR of 5% or more. However, in 99% of the scenarios, the neural network classifier demodulator provided a success rate at least equal to that of the matched filter detector.

TABLE 3. Comparison of the matched filter detector and neural network-classifier demodulator performance for different modulators with AWGN channel.

Modulator Type	Matched filter detector and neural network-classifier demodulator Performance	Reference Figure Number (Training:Test Ratio)
2-PSK	Identical	
4-PSK	Identical	Fig 2 (70:30)
8-PSK	Identical	Fig 3 (60:40)
16-PSK	Identical (except for SNR = 20 dB)	Fig 4 (80:20)
2-QAM	Identical	
4-QAM	Identical	Fig 5 (70:30)
8-QAM	Identical	Fig 6 (60:40)
16-QAM	Identical	Fig 7 (80:20)

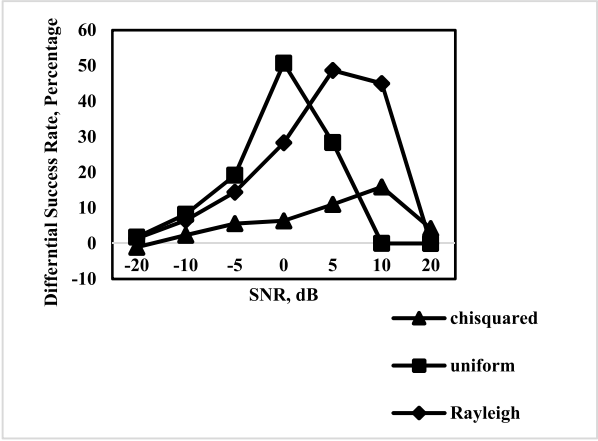

FIGURE 31. The differential of success rate (success rate in percentage for neural-network classifier demodulator - success rate in percentage for matched filter detector) is plotted for 16-QAM for SNR values of −20 dB to 20 dB. The additive chisquared, additive uniform, and additive Rayleigh noise channels are considered. Sample Size, N = 20000. The ratio of training to test data is 70:30.

3) Low SNR detection is important for cognitive radio environments [9], spectrum sensing [10], [11], underwater acoustics [15], infrared point target detection and tracking [17], real-time remote sensing [18], seismic monitoring [19], target detection and tracking [20], and helicopter blade detection [21].

For additive non-Gaussian channels, the neural network classifier demodulator success rate exceeds that of the matched filter detector by 5% or more by

a. 42% for SNR = −20 dB
b. 88% for SNR = −10 dB
c. 100% for SNR = −5 dB
d. 88% for SNR = 0 dB
e. 79% for SNR <= 0 dB

TABLE 4. Comparison of success rate of neural network-classifier demodulator with success rate of matched filter detector for M-PSK, M-QAM for additive non-gaussian noise channel.

Modulator Type	Channel Type	Success Rate (percentage) of neural network-classifier demodulator – Success Rate of Matched filter detector						
		-20 dB	-10 dB	-5 dB	0 dB	5 dB	10 dB	20 dB
2-PSK	Additive chisquared	5.4	8.7	8.9	7.2	4.9	1.7	0.0
4-PSK		14.6	24.1	22.7	19.4	13.1	4.7	0.0
8-PSK		11.6	18.6	19.4	24.2	15.5	11.9	1.6
16-PSK		3.7	3.0	5.7	5.7	7.7	3.7	4.3
2-QAM		5.0	7.4	7.4	7.1	4.6	1.6	0.0
4-QAM		6.6	10.5	12.4	12.9	11.6	6.1	0.2
8-QAM		5.0	4.1	12.2	14.3	16.7	14.2	2.0
16-QAM		-1.1	2.3	5.6	6.4	11.0	15.9	4.2
2-PSK	Additive uniform	6.0	21.8	9.9	0.0	0.0	0.0	0.0
4-PSK		7.3	22.1	30.9	8.7	0.0	0.0	0.0
8-PSK		4.1	15.6	30.6	41.5	8.2	0.0	0.0
16-PSK		2.4	8.5	17.0	27.0	39.7	13.3	-10.7
2-QAM		6.1	22.0	10.2	0.0	0.0	0.0	0.0
4-QAM		4.9	23.6	38.7	0.0	0.0	0.0	0.0
8-QAM		3.0	13.2	27.3	45.6	0.0	0.0	0.0
16-QAM		1.8	8.2	19.2	50.7	28.4	0.0	0.0
2-PSK	Additive Rayleigh	8.3	20.3	25.7	17.3	2.1	0.0	0.0
4-PSK		4.2	13.7	25.0	35.6	23.7	1.2	0.0
8-PSK		2.6	9.1	19.1	35.4	45.0	24.5	0.0
16-PSK		1.0	5.6	10.7	19.8	34.8	43.9	2.7
2-QAM		7.3	19.3	25.7	17.9	2.1	0.0	0.0
4-QAM		5.9	19.8	31.7	40.2	19.7	0.6	0.0
8-QAM		3.6	12.6	22.4	38.0	48.9	22.2	0.0
16-QAM		1.4	6.5	14.4	28.3	48.7	45.0	0.0

f. 63% for SNR = 5 dB
g. 38% for SNR = 10 dB
h. 0% for 20 dB

This suggests that the neural network-classifier demodulator performed better than the matched filter detector for SNR values $\leq$ 0 dB. The classifier performed as well as the matched filter detector in 99% of the scenarios. In fact, 76% of the scenarios in which the success rate for the neural network classifier demodulator exceeded the success rate for the matched filter detector for additive non-Gaussian channels by 5% or

TABLE 5. Range (maximum – minimum) of success rates for various values of N for SNR = −20 dB, 0 dB and M-PSK, M-QAM (M=2, 16).

Modulator Type	Noise Channel type	Range (maximum - Minimum) of Success Rates				
		all N	All N except N=100	All N except N=100, 200	all N except N=100, 200, 1000	N=10000, 20000
2-PSK	SNR=-20 dB, AWGN	7.89	3.5	3.5	0.87	0.06
	SNR = 0 dB, AWGN	15	7.93	1.93	1.4	0.91
	SNR=-20 dB, Additive chisquared	5.83	5.83	2.96	1.49	0.37
	SNR = 0 dB, Additive chisquared	4.86	4.86	2.55	1.37	0.29
	SNR=-20 dB, Additive uniform	19.71	1.69	1.26	1.26	0.8
	SNR = 0 dB, Additive uniform	0	0	0	0	0
	SNR=-20 dB, Additive Rayleigh	5.96	5.96	5.96	1.11	1.11
	SNR = 0 dB, Additive Rayleigh	1.13	1.13	0.46	0.46	0.21
16-PSK	SNR=-20 dB, AWGN	7.9	3.5	3.5	0.87	0.06
	SNR = 0 dB, AWGN	15	7.93	1.93	1.4	0.91
	SNR=-20 dB, Additive chisquared	9.19	9.19	2	0.88	0.14
	SNR = 0 dB, Additive chisquared	10.36	10.36	2.55	0.78	0.38
	SNR=-20 dB, Additive uniform	6.7	2.86	2.01	1.98	1.98
	SNR = 0 dB, Additive uniform	14.62	6.13	6.13	6.13	6.06

TABLE 5. *(Continued.)* **Range (maximum – minimum) of success rates for various values of N for SNR = −20 dB, 0 dB and M-PSK, M-QAM (M=2, 16).**

2-QAM	SNR=-20 dB, Additive Rayleigh	5.69	1.15	0.75	0.75	0.75
	SNR = 0 dB, Additive Rayleigh	21.65	9.53	9.53	3.75	1.2
	SNR=-20 dB, AWGN	8.22	8.22	3.45	1.42	0.21
	SNR = 0 dB, AWGN	10.86	5.70	5.04	0.87	0.87
	SNR=-20 dB, Additive chisquared	5.04	2.03	1.65	1.57	0.57
	SNR = 0 dB, Additive chisquared	16.65	2.97	2.31	1.40	0.25
	SNR=-20 dB, Additive uniform	14.49	1.76	1.76	1.76	1.49
	SNR = 0 dB, Additive uniform	0	0	0	0	0
16-QAM	SNR=-20 dB, Additive Rayleigh	11.15	5.12	3.92	1.18	0.59
	SNR = 0 dB, Additive Rayleigh	2.49	2.16	0.73	0.33	0.22
	SNR=-20 dB, AWGN	8.01	6.51	2.79	0.72	0.72
	SNR = 0 dB, AWGN	16.26	16.26	2.15	1.33	1.33
	SNR=-20 dB, Additive chisquared	5.78	5.78	2.48	2.48	1.96
	SNR = 0 dB, Additive chisquared	17.73	17.73	8.29	8.29	7.01
	SNR=-20 dB, Additive uniform	14.00	4.17	4.17	0.62	0.151
	SNR = 0 dB, Additive uniform	21.24	3.16	2.31	1.27	0.51

TABLE 5. *(Continued.)* **Range (maximum – minimum) of success rates for various values of N for SNR = −20 dB, 0 dB and M-PSK, M-QAM (M=2, 16).**

	SNR=-20 dB, Additive Rayleigh	6.50	1.76	0.69	0.69	0.53
	SNR = 0 dB, Additive Rayleigh	21.13	21.13	1.18	1.18	0.10

TABLE 6. **Pairwise differential success rate for M-PSK, M-QAM and various values of SNR for training:test data ratios 60:40, 70:30, and 80:20 for awgn.**

Modulation Type	Constellation Type, M	Training:Test Ratios	Absolute values of pairwise differential success rate						
			-20 dB	-10 dB	-5 dB	0 dB	5 dB	10 dB	20 dB
2-PSK	2-PSK	60:40-70:30	0.07	0.14	0.09	0.23	0.00	0.00	0.00
		70:30-80:20	0.20	0.17	0.40	0.38	0.03	0.00	0.00
		60:40-80:20	0.13	0.04	0.49	0.15	0.04	0.00	0.00
4-PSK	4-PSK	60:40-70:30	0.30	0.36	0.20	0.08	0.12	0.01	0.00
		70:30-80:20	1.23	1.48	1.49	1.76	0.16	0.05	0.00
		60:40-80:20	1.53	1.84	1.49	1.68	0.27	0.04	0.00
8-PSK	8-PSK	60:40-70:30	0.26	0.38	0.56	1.14	1.29	1.19	0.00
		70:30-80:20	0.00	0.51	0.00	0.00	0.00	0.00	0.00
		60:40-80:20	0.27	0.90	0.56	1.14	1.29	1.19	0.00
16-PSK	16-PSK	60:40-70:30	0.45	0.00	0.32	0.17	0.61	0.55	15.5
		70:30-80:20	0.51	0.08	0.10	0.37	0.41	0.28	0.69
		60:40-80:20	0.06	0.08	0.42	0.20	1.02	0.83	16.2
2-QAM	2-QAM	60:40-70:30	0.05	0.06	0.04	0.11	0.05	0.02	0.00
		70:30-80:20	0.29	0.57	0.34	0.65	0.28	0.01	0.00
		60:40-80:20	0.34	0.63	0.30	0.54	0.23	0.03	0.00
4-QAM	4-QAM	60:40-70:30	1.19	0.47	0.02	0.11	0.02	0.00	0.00
		70:30-80:20	0.63	0.84	0.50	0.03	0.09	0.00	0.00
		60:40-80:20	0.56	0.38	0.52	0.14	0.07	0.00	0.00
8-QAM	8-QAM	60:40-70:30	0.12	0.12	0.20	0.37	0.18	0.05	0.00
		70:30-80:20	0.33	0.08	0.34	0.25	0.09	0.01	0.00
		60:40-80:20	0.45	0.12	0.55	0.63	0.09	0.04	0.00
16-QAM	16-QAM	60:40-70:30	0.08	0.30	0.20	0.00	0.02	0.02	0.00
		70:30-80:20	0.09	0.05	0.03	0.15	0.02	0.01	0.00
		60:40-80:20	0.17	0.36	0.17	0.14	0.00	0.01	0.00

more corresponded to noise channels with SNR $\leq$ 0 dB. However, even for a higher SNR, the proposed demodulator performs as well as, or better than, the matched filter detector.

4) The success rate of the proposed demodulator exceeded that of the matched filter detector by 5% or more for 62% of M-PSK scenarios and 57% of M-QAM scenarios. The performance of the neural network classifier demodulator is independent of the constellation type.
5) The success rate of the neural network classifier demodulator, which exceeded that of the matched filter detector by 5% or higher, was observed in 50% of the scenarios listed in Table 4, for which M=2, independent of whether PSK or QAM was used. This measure of superior performance occurred in 62% of the M=4 constellations, 64% of the M=8 constellations, and 62% of the M=16 constellations, respectively. Thus, superior performance has a bias for M values greater than two.
6) 35%, 28%, and 37% of the 100 scenarios, where the success rate of the neural network classifier demodulator exceeded the success rate of the matched filter detector by 5% or higher for the additive chisquared noise channel, additive uniform noise channel, and additive Rayleigh noise channel, respectively. The performance of the proposed demodulator was superior for the additive chisquare and Rayleigh noise channels.

The performance of the NN classifier is identical to that of the MFD for all AWGN channels and SNR levels considered in this study (Fig 2 - Fig 7), including 0 dB and lower, and for different constellation types, constellation sizes, or training-to-test data ratios. A sample size of 20000 was used for the simulations.

MFD is optimal for the AWGN channel [12], [14] and as evidenced by the NN classifier-demodulator having the same success rates as the MFD for various scenarios with the AWGN channel (Table 2). Prior studies and simulations [15], [16] have established that MFD is not optimal for non-Gaussian noise channels, and this is confirmed in this study for chisquared, uniform, and Rayleigh noise channels. Overall, for the non-Gaussian noise channels, the performance of the NN classifier is superior to the performance of MFD in 78.5% of the scenarios and identical in 20.5% of the scenarios. Lower performance and marginally lower performance were observed in 1% of scenarios. The NN classifier demonstrated superior performance over MFD in the following specific scenarios. There is equality of performance in a few scenarios, particularly at higher SNR levels.

1) Chisquared noise channel, PSK modulation, M = 2, 4, 8, and 16; training-to-test data ratio of 70:30; sample size N=20000; chosen classifier parameters (Table 2): superior performance in 93% of scenarios and equality in the remaining scenarios (Table 4).

2) Chisquared noise channel, QAM, M = 2, 4, 8, and 16; training-to-test data ratio of 70:30; sample size N=20000; chosen classifier parameters (Table 2): superior performance in 93% of scenarios and equality in 3.5% of the scenarios (Table 4). Marginally lower performance was observed in 3.5% of the scenarios.

3) Uniform noise channel, PSK modulation, M = 2, 4, 8, and 16; training-to-test data ratio of 70:30; sample size N=20000; chosen classifier parameters (Table 2). For SNR = 20 dB, the success rate of the classifier is lower than that of the MFD: superior performance in 68% of the scenarios and equality in 28.5% of the scenarios (Table 4). Lower performance was observed in 3.5% of the scenarios.

4) Uniform noise channel, QAM, M = 2, 4, 8, and 16; training-to-test data ratio of 70:30; sample size N=20000; chosen classifier parameters (Table 2): superior performance in 57% of the scenarios and equality in 43% of the scenarios (Table 4).

5) Rayleigh noise channel, PSK modulation, M = 2, 4, 8, and 16; training-to-test data ratio of 70:30; sample size N=20000; chosen classifier parameters (Table 2). For SNR = 20 dB, success rate of classifier is lower than MFD: superior performance in 89% of the scenarios and equality in 11% of the scenarios (Table 4).

6) Rayleigh noise channel, QAM, M = 2, 4, 8, and 16; training-to-test data ratio of 70:30; sample size N=20000; chosen classifier parameters (Table 2): superior performance in 82% of the scenarios and equality in 18% of the scenarios (Table 4).

It can be inferred from Table 4 that the classifier-demodulator was superior to MFD in 97% of the scenarios and marginally lower in 3% of the scenarios with additive chisquared noise channel and SNR $\leq$ 0dB. The performance of the classifier-demodulator was superior to MFD in 91% of the scenarios and equal to that of MFD in 9% of the scenarios with additive uniform noise channel and SNR $\leq$ 0dB. With a Rayleigh noise channel and SNR $\leq$ 0dB, the NN classifier-demodulator exhibits superior performance in 100% of the scenarios.

The NN-classifier demodulator exhibits superior performance over MFD, specifically for non-Gaussian noise channels and particularly for SNR values of 0 dB or less. Non-Gaussian noise channels are more likely to occur in practical environments and settings. Further, multiple applications such as spectrum sensing, cognitive radio networks and remote sensing require the receiver to operate in environments with SNR $\leq$ 0 DB.

Fig 31 is derived from Table 4 for 16-QAM. The performance of the proposed demodulator was superior to that of the matched filter detector in all noise channel scenarios for 16-QAM, except for the case of SNR = -20 dB for the additive chisquared noise channel. It was further observed that the performance of the neural network classifier demodulator exceeded that of the matched filter detector by 5% or more for almost all SNR values when the noise channel was additively uniform or Rayleigh. It is significant that at SNR = 0 dB, the success rate of the NN classifier-demodulator operating on the uniform noise channel exceeded the success rate of MFD by 50.7 percentage points. Similarly, for SNR = 5 dB and 10 dB, the success rate of the classifier-demodulator exceeded the MFD success rate, by 48.7 and 45, respectively. For 0 dB or lower noise channels, the neural network classifier

performs best in a uniform noise channel, whereas for higher SNR values, the proposed demodulator performs best in a Rayleigh noise channel.

In Table 5, the range of success rates is calculated for various sample sizes. For example, the first column considers all sample size values ("All N") implying N ϵ {100, 200, 1000, 5000, 10000, 20000} while the third column ("All N except N = 100, 200") refers to N ϵ {1000, 5000, 10000, 20000}. The set of appropriate sample sizes was the set of sample sizes with the smallest range. The ad hoc 5% is a measure of the variability of the range. The following inferences can be made from this table:

1) It was observed that when all values of N (100, 200, 1000, 5000, 10000, and 20000) were considered, the range of success, calculated as the difference between the maximum and minimum success rates for the particular choice of constellation type, value of M, value of SNR, and choice of noise channel (AWGN, chisquared, uniform, or Rayleigh), exceeded 5% in 84% of the scenarios.
2) When N=100 was excluded, the range of success rates exceeded 5% in 50% of scenarios.
3) When N=100 and N=200 were excluded, the range of success rates exceeded 5% in 16% of scenarios.
4) When only N=5000, N=10000, and N=20000 were included, the range of success rates exceeded 5% in 6% of scenarios.
5) When only N=10000 and N=20000 were included, the range of success rates exceeded 5% in 6% of scenarios.
6) With the PSK constellation, the range of success rates exceeded 5% in 50% of scenarios.
7) With the QAM constellation, the range of success rates exceeded 5% in 50% of scenarios.
8) With SNR = − 20 dB across constellation types, the range of success rates exceeded 5% in 46% of scenarios.
9) With SNR = 0 dB across constellation types, the range of success rates exceeded 5% in 54% of scenarios.
10) With M=2 across constellation types, the range of success rates exceeded 5% in 37% of scenarios.
11) With M=16 across constellation types, the range of success rates exceeded 5% in 63% of scenarios.

The sample size N is a key parameter that influences the success rate and reliability of the classifier demodulator. The sample size was not significantly influenced by constellation type (PSK or QAM). The range of success rate values decreased for a given SNR value (−20 dB, 0 dB), noise channel type (additive chisquare, uniform, and Rayleigh), and constellation (2-PSK, 16-PSK, 2-QAM, and 16-QAM). For example (Table 5), the range reduced from 5.83 when the complete set of sample sizes were considered for 2-PSK, -20 dB, and additive chisquare noise channel, to 0.37 differential success rate when only N = 10000, 20000 were considered. Similarly, the range reduced from 21.13 when the complete set of sample sizes was considered for 16-QAM, 0 dB, and additive Rayleigh noise channel to 0.10 differential success rate when only N = 10000 and 20000 were considered. The sample size was selected using the thumb rule of 5% significance in the range of values for any given constellation and noise channel. For M = 16, a sample size of 20000 is appropriate because the range is 6.06 for 16-PSK, 0 dB, and an additive uniform channel for the sample size set of {10000 and 20000}. Similarly, for 16-QAM, 0 dB, and additive chisquare noise, the range is 7.01 for the sample size set of {10000, 20000}. For all other scenarios, sample sizes of 5000, 10000, and 20000 can be selected because for this sample size set under all other constellation types and sizes, SNR levels, and noise channel types, the range was less than 5%.

The ratio of the standard deviation to the mean (coefficient of dispersion) of the success rate can also be used to measure dispersion to study the impact of the sample size on the performance of the NN classifier. This ratio is more reliable and robust than the range. The ratios presented here are the average success rates for two sets of sample sizes: {N = 5000, 10000, 20000} and {N = 10000, 20000}. In most cases, this ratio is higher for the −20 dB SNR than for 0 dB SNR; the exception is 16-QAM, where the ratio is higher for 0 dB SNR. The ratio is found to be less than 0.1 for 2-PSK and 2-QAM, while for 16-PSK it is approximately 0.9 for -20 dB SNR and around 0.51 for 0 dB SNR. Surprisingly, it is less than 0.17 for the 16-QAM and −20 dB SNR noise channels, and close to 0.3 for the same constellation and 0 dB SNR noise channel. For the AWGN channel and -20 dB SNR level, the ratio is approximately 0.43, whereas for the same channel type and 0 dB SNR level, the ratio is less than 0.07. For the non-Gaussian channels, the ratio ranges from about 0.7 to around 0.75 for -20 dB SNR level and the ratio ranges from 0.33 to 0.48 for 0 dB SNR level. Clearly, there is greater variability for the non-Gaussian channels and 16-PSK. The difference in the corresponding ratios (coefficients of dispersion) for the two sample sets did not exceed 10%. However, it should be noted that the variance and mean were calculated over 8 to 12 samples, which is rather small, with limited reliability of the calculated coefficient of dispersion value.

In conclusion, a sample size of N = 20000 is necessary for M = 16, where all other scenarios N = 5000 or higher, are appropriate. This sample size choice was independent of the selected constellation type and SNR value.

The performance of the proposed demodulator for M-PSK modulation and M-QAM over different Training:Test data ratios is presented in Table 6. The performance of an AWGN channel with a sample size of N = 20000 and various SNR values were compared. The difference in success rate was computed pairwise for three ratios: 60:40, 70:30, and 80:20. The largest difference in the success rate for M-PSK, excluding 16-PSK, for an SNR of 20 dB was 1.84%. The largest difference in the success rate of the M-QAM was 1.19%. For 16-PSK and 20 dB, the difference in the success rate between the 70:30 and 80:20 ratios was 0.686%, whereas the other

two differences exceeded 15%. A training-to-test data ratio of 70:30 or 80:20 is appropriate.

IV. CONCLUSION

The success rate of a neural network classifier (rectified linear unit rectification unit, 10 layers, softmax output layer activation)-based demodulator was proposed and evaluated for phase-shift keying (PSK) and quadrature amplitude modulation (QAM)-modulated signals corrupted by additive white Gaussian noise with an SNR ranging from -20 dB to +20 dB. The message signal consists of uniformly distributed pseudo-random integers. The matched filter detector was optimal for the AWGN noise channel. However, it is clear that the NN-based classifier demodulator performs as well as the optimal detector does in the AWGN channel.

The methodology for determining the feasibility of the classifier demodulator used in this study is outlined as follows. The performance of the NN classifier was studied for AWGN, chisquared, uniform, and Rayleigh noise channels for SNR levels of -20, -10, -5, 0, 5, 10, and 20 dB. The performance of the NN classifier was established for two modulation types (PSK and QAM) and for constellation sizes M = 2, 4, 8, and 16. *First* the performance measure appropriate for the proposed demodulator was selected. In the *second*step, the sample size was determined through independent simulations for sample sizes N=100, 200, 1000, 5000, 10000, and 20000 for SNR = -20 dB and 0 dB for all noise channel types to determine a suitable sample size. A more rigorous analysis of the variations in success rates led to the conclusion that a sample size of 20000 is suitable for M=16, while sample sizes of 5000, 10000, and 20000 were suitable for all other combinations of constellation type (PSK, QAM), value of M (2 and 16), SNR level (-20 dB and 0 dB), and channel types (AWGN and non-Gaussian). *Third*, the training-to-test data ratio selection was determined based on the success rates for the AWGN channel for M-PSK and M-QAM and M=2, 4, 8, and 16. A ratio of 70:30 or 80:20 is recommended. The sample size, N, was set to 20000 to selecting the ratio.

The success rate is calculated as the number of symbols successfully demodulated by the classifier, and is presented as a percentage of the total number of symbols transmitted. The success rate defined in this study is similar to the Symbol Error Rate rather than the bit error rate when measuring the performance of the NN-based classifier solution. The success rate is a more macro-level measure of the performance of a demodulator than the bit error rate and is better suited for the classifier demodulator, where information is transmitted and received in the form of symbols. A macro-level measure of performance is better correlated with system-level requirements. Variations at the micro level may have a limited impact on macro-level performance measures. A 5% measure of significance was used to analyze the differences in success rates.

It is observed that, independent of the constellation type (PSK, QAM), the performance of the NN classifier demodulator recognizes features in the data and performs as well as MFD for the AWGN channel. It is observed that for both PSK and QAM, the performance, in terms of success rate, is the highest for M = 2, slightly lower for M = 4, and least for M = 16, for a given combination of signal, modulation, channel, and classifier parameters. This pattern is observed across noise channel types (AWGN, chisquared, uniform, and Rayleigh) and SNR levels from -20 dB to 20 dB considered in this study, with the exception of the equality of success rates in some noise level scenarios. In some scenarios, the success rate of the classifier demodulator was lower than the MFD success rate.

The performance of the neural network classifier was also compared to that of non-Gaussian channels: additive chisquared, additive uniform, and additive Rayleigh channels, because the matched filter is not optimal for non-Gaussian distributions. This classifier-demodulator performance was compared with the corresponding performance of the M-PSK and M-QAM demodulators (matched filter detection).

The classifier performance was evaluated with respect to channel noise, modulation type (PSK or QAM), constellation type, constellation size (M=2, 4, 8, 16), sample size, and training-to-test data ratio. A key parameter that influences the success rate and reliability of the classifier demodulator is the training-to-test ratio. A ratio of 70:30 or 80:20 is recommended for the parameters considered in this study. With this selection, the range of the absolute differential success rate was less than 2% for all scenarios. This recommendation is independent of the constellation type, size, or SNR value. The neural network classifier performance has a similar dependence on the constellation type (M-PSK or M-QAM) to that of the matched filter detector. The superior performance of the NN classifier demodulator is more pronounced for M = 4, M = 8, and M = 16. For M = 16, a sample size of 20000 is appropriate, whereas for all scenarios, sample sizes of 5000, 10000 or 20000 can be selected. For every type of additive non-Gaussian channel, the neural network-based demodulator outperformed the matched filter detector in many scenarios. The superior performance of the proposed classifier demodulator occurred more frequently for the additive chisquare and Rayleigh noise channels.

The classifier demodulator had a performance equal to or better than MFD in 99% of the scenarios. The classifier performances of M-PSK and M-QAM are comparable. The superior performance of the NN classifier is more pronounced for M $\geq$ 2. A higher success rate was obtained for additive chisquare and Rayleigh noise channels. The proposed demodulator performed significantly better than the matched filter detector for SNR values of $\leq$ 0 dB. The classifier demodulator performed better than MFD by 5% or higher success rate in 100% of scenarios with SNR = -5 dB and 88% of scenarios for SNR = -10 dB and 0 dB. Overall, the proposed demodulator performed better than MFD by 5% or higher in 79% of scenarios for SNR $\leq$ 0 dB. 16-QAM over

an additive uniform noise channel has a better success rate for an SNR of 0 dB or less, whereas 16-QAM over an additive Rayleigh noise channel has a better success rate for an SNR of 5 dB or higher.

Both the matched filter detector and NN-based classifier demodulator performance for the additive chisquared channel and additive uniform channel exceeded the performance of the detectors for the AWGN channel, except for 16-QAM, for many SNR values. It is further observed that both the matched filter detector and NN-based classifier demodulator performance for the AWGN channel lie between those of the NN-based classifier and matched filter detector for the Rayleigh channel, except for 16-QAM, for many SNR values.

For 16-QAM with an SNR $\leq$ 0 dB, the highest success rates were observed when an additive uniform channel was used, whereas for an SNR $\geq$ 5 dB, the highest success rates were observed when an additive Rayleigh channel was used. The pattern and relationships of the plots observed for 16-QAM for the differential success rate against SNR for additive chisquared, uniform, and Rayleigh noise channels were observed for all M-PSK and M-QAM (M = 2, 4, 8, and 16) with differences only in amplitude. Further, it is also observed when comparing the data for success rates for 2-PSK, 4-PSK, 8-PSk, 16-PSK, 2-QAM, 4-QAM, and 8-QAM for AWGN, additive chisquare, additive uniform, and additive Rayleigh noise channels for SNR levels from -20 dB to +20 dB, the performance of the classifier demodulator for each of the non-Gaussian noise channel scenarios is approximately superior to the AWGN channel scenarios. The only exception is 16-QAM, for which the AWGN scenario performance is superior to each non-Gaussian channel scenario. These observations suggest a correlation between the noise distribution and the signal symbol generation distribution, along with the distance measures implicitly used in the neural network classifier.

Although there are differences in the performance of the classifier-demodulator over different non-Gaussian channels, the proposed demodulator is superior to the performance of the MFD. Most real-world noise channels do not have AWGN characteristics, but tend to have some measure of non-Gaussian characteristics. Underwater acoustic noise [15] and snapping shrimp-dominated ambient noise [16], discussed earlier, are two such examples. A demodulation method that is blind to the nature of noise channel distribution characteristics, or at least capable of implicitly detecting the features of the noise channel as part of the method, is certainly useful. The classifier demodulator has demonstrated potential in this study to have this ability to perform well without explicit knowledge of the noise distribution function. In other words, no explicit design is required in the receiver for different noise channel distributions or varying noise channels for then, in principle, a different receiver would be required for each such noise channel distribution.

Broadly speaking, the NN classifier performance is superior to that of the MFD for all non-Gaussian noise channels. The proposed demodulator performs exceptionally well at SNR $\leq$ 0 dB. The NN classifier has the marks of a robust demodulator in channels with varying noise channel distributions and SNR levels, especially SNR $\leq$ 0 dB. This makes it a strong candidate for spectrum sensing, cognitive radio networks, remote sensing, and non-Gaussian channel noise, which are appropriate for underwater acoustics and snapping shrimp-dominated environments.

The classifier performance for different modulation schemes (PSK and QAM) indicates the potential that can be further explored for modulation schemes built upon or built around PSK and QAM. There is a measure of the independence of the classifier on the constellation type, but exceptions and variability across sample sizes require further investigation. The fact that the classifier-demodulator is independent of the modulation type is a reflection of the fact that the classifier implicitly detects the features of the modulation scheme as part of the method. Because 4G and 5G use Orthogonal Frequency Division Multiplexing (OFDM), which builds on variations of QAM and PSK, the classifier demodulator could perform well in 4G and 5G system environments but needs further study. This could lead to the development of an NN-based demodulator in 6G.

For AWGN channels or channels that are close to AWGN, the NN-based demodulator provides a demodulator solution that requires a far less complex or mathematical design than an MFD-based demodulator. A simpler receiver solution is thus possible for M-PSK and M-QAM modulation with M = 2, 4, 8, and 16 or OFDM, which builds on variations of M-PSK or M-QAM. This can result in a less expensive receiver solution. Therefore, a more thorough feasibility study is needed.

The classifier modulator performs as well as the MFD for AWGN channels, independent of the modulation type (PSK or QAM). The SNR levels can fluctuate because the noise distributions can vary owing to the changing environmental and climatic conditions. The enhanced success rate observed for the proposed NN demodulator for SNR levels $\leq$ 0 dB and non-Gaussian noise channel types is interesting. Can this demodulator adapt to dynamically varying noise distributions with distributions varying between AWGN, slightly non-Gaussian, and heavily non-Gaussian distributions? In other words, this single demodulator can adapt to varying noise levels and perhaps varying noise distributions. It would be useful to explore whether a single NN demodulator can work well across a range of SNR levels without redesigning the demodulator. Such a demodulator is adaptive, robust, and cost-effective.

ACKNOWLEDGMENT

The author would like to thank Dr. D. H. Johnson, Rice University, Houston, TX, USA, for his valuable email input and discussions. He also thank Amity University Dubai for the use of these facilities and the anonymous reviewers for their invaluable feedback.

REFERENCES

[1] Z. Qin, H. Ye, G. Y. Li, and B. F. Juang, "Deep learning in physical layer communications," *IEEE Wireless Commun.*, vol. 26, no. 2, pp. 93–99, Apr. 2019, doi: 10.1109/MWC.2019.1800601.
[2] N. Farsad, M. Rao, and A. Goldsmith, "Deep learning for joint source-channel coding of text," in *Proc. IEEE Int. Conf. Acoust., Speech Signal Process. (ICASSP)*, Apr. 2018, pp. 2326–2330.
[3] H. Kim, S. Oh, and P. Viswanath, "Physical layer communication via deep learning," *IEEE J. Sel. Areas Inf. Theory*, vol. 1, no. 1, pp. 5–18, May 2020, doi: 10.1109/JSAIT.2020.2991562.
[4] J. Shi, S. Hong, C. Cai, Y. Wang, H. Huang, and G. Gui, "Deep learning-based automatic modulation recognition method in the presence of phase offset," *IEEE Access*, vol. 8, pp. 42841–42847, 2020, doi: 10.1109/ACCESS.2020.2978094.
[5] S. Liu, T. Wang, and S. Wang, "Toward intelligent wireless communications: Deep learning–based physical layer technologies," *Digit. Commun. Netw.*, vol. 7, no. 4, pp. 589–597, Nov. 2021, doi: 10.1016/j.dcan.2021.09.014.
[6] M. Honkala, D. Korpi, and J. M. J. Huttunen, "DeepRx: Fully convolutional deep learning receiver," 2021, *arXiv:2005.01494v2*.
[7] J. Hoydis, F. A. Aoudia, A. Valcarce, and H. Viswanathan, "Toward a 6G AI-native air interface," *IEEE Commun. Mag.*, vol. 59, no. 5, pp. 76–81, May 2021, doi: 10.1109/MCOM.001.2001187.
[8] T. O'Shea and J. Hoydis, "An introduction to deep learning for the physical layer," *IEEE Trans. Cognit. Commun. Netw.*, vol. 3, no. 4, pp. 563–575, Dec. 2017, doi: 10.1109/TCCN.2017.2758370.
[9] J. J. Popoola and R. van Olst, "Application of neural network for sensing primary radio signals in a cognitive radio environment," in *Proc. IEEE Africon*, Victoria Falls, Zambia, Sep. 2011, pp. 1–6, doi: 10.1109/AFRCON.2011.6072009.
[10] Y. Zhang, P. Wan, S. Zhang, Y. Wang, and N. Li, "A spectrum sensing method based on signal feature and clustering algorithm in cognitive wireless multimedia sensor networks," *Adv. Multimedia*, vol. 2017, pp. 1–10, Oct. 2017, doi: 10.1155/2017/2895680.
[11] Y. Lu, P. Zhu, D. Wang, and M. Fattouche, "Machine learning techniques with probability vector for cooperative spectrum sensing in cognitive radio networks," in *Proc. IEEE Wireless Commun. Netw. Conf.*, Doha, Qatar, Apr. 2016, pp. 1–6, doi: 10.1109/WCNC.2016.7564840.
[12] O. Zeitnouni, J. Ziv, and N. Merhav, "When is the generalized likelihood ratio tes optimal?" *IEEE Trans. Inf. Theory*, vol. 38, no. 5, pp. 1597–1602, Sep. 1992.
[13] M. Viswanathan. *How to Generate AWGN Noise in Matlab/Octave(Without Using in-built AWGN Function)*. Accessed: Nov. 2023. [Online]. Available: https://www.gaussianwaves.com/gaussianwaves/wp-content/uploads/2015/06/How_to_generate_AWGN_noise.pdf
[14] G. Turin, "An introduction to matched filters," *IEEE Trans. Inf. Theory*, vol. IT-6, no. 3, pp. 311–329, Jun. 1960, doi: 10.1109/tit.1960.1057571.
[15] Y. Y. Al-Aboosi, H. A. Taha, and H. A. Abdualnabi, "Locally optimal detection of signals in underwater acoustic noise with student's t-distribution," *IOP Conf. Ser., Mater. Sci. Eng.*, vol. 433, Nov. 2018, Art. no. 012086, doi: 10.1088/1757-899x/433/1/012086.
[16] M. A. Chitre, J. R. Potter, and S.-H. Ong, "Optimal and near-optimal signal detection in snapping shrimp dominated ambient noise," *IEEE J. Ocean. Eng.*, vol. 31, no. 2, pp. 497–503, Apr. 2006, doi: 10.1109/JOE.2006.875272.
[17] L. Jia, P. Rao, Y. Zhang, Y. Su, and X. Chen, "Low-SNR infrared point target detection and tracking via saliency-guided double-stage particle filter," *Sensors*, vol. 22, no. 7, p. 2791, Apr. 2022, doi: 10.3390/s22072791.
[18] T. J. Ma and R. J. Anderson, "Remote sensing low signal-to-noise-ratio target detection enhancement," *Sensors*, vol. 23, no. 6, p. 3314, Mar. 2023, doi: 10.3390/s23063314.
[19] R. R. Leach, F. U. Dowla, and C. A. Schultz, "Optimal filter parameters for low SNR seismograms as a function of station and event location," *Phys. Earth Planet. Interiors*, vol. 113, nos. 1–4, pp. 213–226, Jun. 1999, doi: 10.1016/s0031-9201(99)00006-0.
[20] N. Amrouche, A. Khenchaf, and D. Berkani, "Detection and tracking targets under low SNR," in *Proc. IEEE Int. Conf. Ind. Technol. (ICIT)*, Toronto, ON, Canada, Mar. 2017, pp. 992–996, doi: 10.1109/ICIT.2017.7915496.
[21] D. D. Nguyen, S. T. N. Nguyen, R. Melino, S. Kodituwakku, and H. Tran, "Radar detection of helicopters at low SNR using time-frequency transforms," Univ. Adelaide, Adelaide, SA, Australia, Tech. Rep. DST-Group-TR-3481, 2018. [Online]. Available: https://www.dst.defence.gov.au/sites/default/files/publications/documents/DST-Group-TR-3481.pdf

ANAND KUMAR (Senior Member, IEEE) received the degree in electrical and electronics engineering from BITS Pilani, Rajasthan, India, in 1983, and the M.S. and Ph.D. degrees in electrical and computer engineering from Rice University, Houston, TX, USA, in 1986 and 1990, respectively.

He was with the Central Research Laboratory and British Physical Laboratories. His experiences include stints at Motorola and Ericsson. He worked on the Iridium Project. He was also with the Higher Colleges of Technology, New York Institute of Technology, and BITS Pilani. He is currently a Professor with Amity University Dubai. His roles include the Project Manager, the Product Manager, the Dean, an Associate Dean, and the Head of Department. He has several peer-reviewed and Scopus indexed publications to his credit. He has supervised Ph.D. students. His current research interests include deep learning applications in the physical layer of communication systems and innovations in teaching and learning.

Dr. Kumar has organized three conferences, technically co-sponsored by IEEE, as the chair/co-chair.